Original Research

Left Ventricular Infarct Size, Peri-Infarct Zone, and Papillary Scar Measurements: A Comparison of High-Resolution 3D and Conventional 2D Late Gadolinium Enhancement Cardiac MR

Dana C. Peters, PhD,[1,2]* Evan A. Appelbaum, MD,[1,2] Reza Nezafat, PhD,[1,2]
Basem Dokhan, BS,[3] Yuchi Han, MD,[1,2] Kraig V. Kissinger, RT,[1]
Beth Goddu,RT, [1] and Warren J. Manning, MD[1,2,4]

Purpose: To compare higher spatial resolution 3D late gadolinium enhancement (LGE) cardiovascular magnetic resonance (Cardiac MR) with 2D LGE in patients with prior myocardial infarction.

Materials and Methods: Fourteen patients were studied using high spatial resolution 3D LGE ($1.3 \times 1.3 \times 5.0 \ mm^3$) and conventional 2D LGE ($2 \times 2 \times 8 \ mm^3$) scans. The signal-to-noise ratio (SNR) and contrast-to-noise ratio (CNR) were measured. Total infarct volume, peri-infarct volume measured in a limited slab, and papillary muscle scar volume were compared using Bland–Altman analysis. Image quality was graded.

Results: 3D LGE had higher scar SNR ($P < 0.001$), higher myocardial SNR ($P = 0.001$), higher papillary scar-blood CNR ($P = 0.01$), and greater sharpness ($P = 0.01$). The scar volumes agreed (14.5 ± 8.2 for 2D, vs. 13.2 ± 8.8 for 3D), with bias ± 2 standard deviations (SDs) of 0.5 ± 6.8 mL, $P = 0.59$ R = 0.91. The peri-infarct volumes correlated but less strongly than scar ($P = 0.40$, R = 0.77). For patients with more heterogeneous scar, larger peri-infarct volumes were measured by 3D (1.9 ± 1.1 mL for 2D vs. 2.4 ± 1.6 mL for 3D, $P = 0.15$, in the matched region). Papillary scar, present in 6/14 (42%) patients, was more confidently identified on 3D LGE.

Conclusion: Higher spatial resolution 3D LGE provides sharper images and higher SNR, but less myocardial nulling. Scar volumes agree well, with peri-infarct volumes correlating less well. 3D LGE may be superior in visualization of papillary muscle scar.

LATE GADOLINIUM ENHANCEMENT (LGE) cardiovascular magnetic resonance (Cardiac MR) is the gold standard for noninvasive imaging of myocardial fibrosis (1,2). Due to the efficacy of implantable cardioverter defibrillators (ICD) and ventricular tachycardia (VT) ablation therapies in preventing sudden death, there is increased interest in improved risk-assessment for those with arrhythmic substrate (prior infarct/scar). Several studies have demonstrated that arrhythmias and mortality are related to increased infarct and peri-infarct zone (or "gray zone") volumes (3–6), as measured by LGE. The presence of scar, independent of its size, also predicts future adverse outcomes (7). Increased spatial resolution may more accurately represent scar morphology and the peri-infarct zone and identify small areas of fibrosis such as papillary muscle infarcts. Papillary muscles that are heterogeneously scarred have been observed to be sites of ventricular arrhythmias after myocardial infarction (8–10). Identification of small areas of scar and improved measurement of peri-infarct zones would increase the value of the LGE test.

While 2D breath-hold LGE is most commonly used for clinical imaging, several studies have presented good quality results using 2D free-breathing (11), 3D breath-hold (12–14), or 3D free-breathing (15,16) techniques. However, those efforts focused on alternative methods for those patients who cannot perform repeated breath-holding. We sought to compare a higher

spatial resolution free-breathing 3D LGE approach with our clinical 2D LGE method for visualizing smaller areas of scar and measuring LGE volume.

MATERIALS AND METHODS

Imaging

Between January 2007 and March 2009, we enrolled 36 patients referred for LGE scanning for suspected myocardial infarction. The study was approved by the hospital committee on clinical investigations. All imaging was performed on a 1.5 T Philips Achieva Cardiac MR scanner (Philips HealthCare, Best, Netherlands), equipped with a 5-element phased-array cardiac coil. The MR exam included assessment of cardiac function, flow, anatomy, and viability. Left ventricular (LV) ejection fraction (EF), mitral regurgitation fraction, and LV dimensions as measured by cardiac MR were obtained. 2D breath-hold LGE short-axis images were acquired ≈15 minutes after injection of 0.2 mmol/kg Gd-DTPA (Magnevist, Schering, Berlin, Germany), followed by 3D free-breathing LGE short-axis imaging. Imaging parameters for the 2D LGE were: 2D spoiled gradient echo inversion recovery, with 160×160 matrix, 320 cm field of view (FOV), 8 mm slices, with 2 mm gaps, TR/TE/α = 4.3msec/1.5msec/20°, 40 views per segment, receiver bandwidth (RBW) = ± 30.6 kHz, partial echo, fat saturation, one RR between inversions, two signal averages (2 NSA). An average of 12 ± 1.5 slices are acquired, each in eight heart-beat breath-holds, with average total scan time (including time between breath-holds) of $6:18 \pm 1:40$ minutes. ECG-triggering in late-diastole and breath-holding were used to reduce motion artifacts. The imaging parameters for the free-breathing 3D LGE sequence were similar, except: 256×224-208 Ny $\times$ 23–32 (28 ± 3) Nz matrix (before zero-filling), TR/TE/α = 5.7msec/2.7msec/25°, 26 views per segment, RBW = ± 34.7 kHz full echoes, 1 signal average, with ECG-triggering and navigator-gating (5 mm window, no tracking) to reduce motion artifacts, phase-encoding direction: foot-head. The average nominal scan time was $3:29 \pm 0:32$ minutes (assuming a 60 bpm heart-rate), with average total scan time of $6:58 \pm 1:45$ minutes with $52 \pm 10\%$ navigator efficiency. For both the 2D and 3D LGE sequences, a Look–Locker (17) sequence was used prior to both imaging sequences to choose the best inversion time. The average TI was 255 ± 32 msec for 2D LGE, and 269 ± 33 msec for 3D LGE.

The true spatial resolutions of the 2D and 3D LGE acquisitions were $2 \times 2 \times 8$ mm^3 and $1.3 \times 1.4 \times 5$ mm^3, respectively, with reconstructed spatial resolutions of $1.2 \times 1.2 \times 8$ mm^3 and $0.62 \times 0.62 \times 2.5$ mm^3, respectively.

Analysis

Signal-to-noise ratio (SNR) was measured in the slice with the most prominent scar, using signal intensity in the region of interest (ROI) in the LV myocardial LGE, papillary LGE, remote myocardium, and blood, divided by the standard deviation (SD) of the signal intensity in the air-space anterior to the chest wall. Contrast-to-noise ratio (CNR) was the difference of SNR of the two tissues. SNR of the 2D and 3D LGE images was also measured in a phantom consisting of Gd-DTPA-doped water (T1s of 440, 330, and 300 msec, representing myocardium, blood, and scar, respectively).

Scar Measurement

To quantify LGE, which indicates scar, endocardial and epicardial myocardial borders were manually drawn on all short-axis slices for each subject using a commercial cardiac software package (ViewForum 5.1, Philips). After measuring the peak LGE signal in the images, scarred myocardium was identified as having signal >50% of the peak LGE signal (the "full width half maximum technique") (6,18). Peri-infarct volumes were measured on single slice of the 2D LGE images (10 mm effective slice thickness) with LGE and the matching 3D LGE slices (four 2.5 mm slices). The peri-infarct zone comparisons were limited to a single 2D slice to reduce errors in the measurement introduced if endocardial or epicardial contours are not drawn to exclude nonmyocardial regions. Peri-infarct regions were identified as myocardium with signal > maximum signal in normal myocardium, but below the cutoff for scar, as previously described (6,18). Figure 1 shows examples of 2D and 3D images, with endocardial and epicardial contours, and the resulting volumes using the two thresholds for scar and peri-infarct zone. To quantify combined papillary muscle and trabecular scar, high signal intensity in the LV cavity was manually traced using ROIs.

Subjective Evaluation

Images were visually graded a scale of 1 to 4 (1 = poor, 2 = average, 3 = good, 4 = excellent) for myocardial/scar and endocardial sharpness, contrast (myocardial nulling and scar/blood contrast), and overall quality by two independent observers, each with >5 years of Cardiac MR experience. The 3D and 2D LGE images were visually graded as having an apparent visual heterogeneous or homogeneous LGE structure. The presence or absence of papillary muscle LGE and the confidence of the decision (high or low) were noted for each dataset.

Statistics

Continuous data are presented as mean ± SD. For comparison of LGE volumes, Bland–Altman analysis was performed. The 3D and 2D SNRs and volumes were compared using paired *t*-tests, and unpaired *t*-tests to compare data between patients with and without papillary muscle scar. Categorical variables (ie, image quality scores) were compared with Wilcoxon signed rank test. The chi-square test was used to compare proportions. A two-sided *P*-value <0.05 was considered significant. All statistics were performed in Microsoft Office Excel 2003 statistics package, or with Stata IC 10 (StataCorp, College Station, TX).
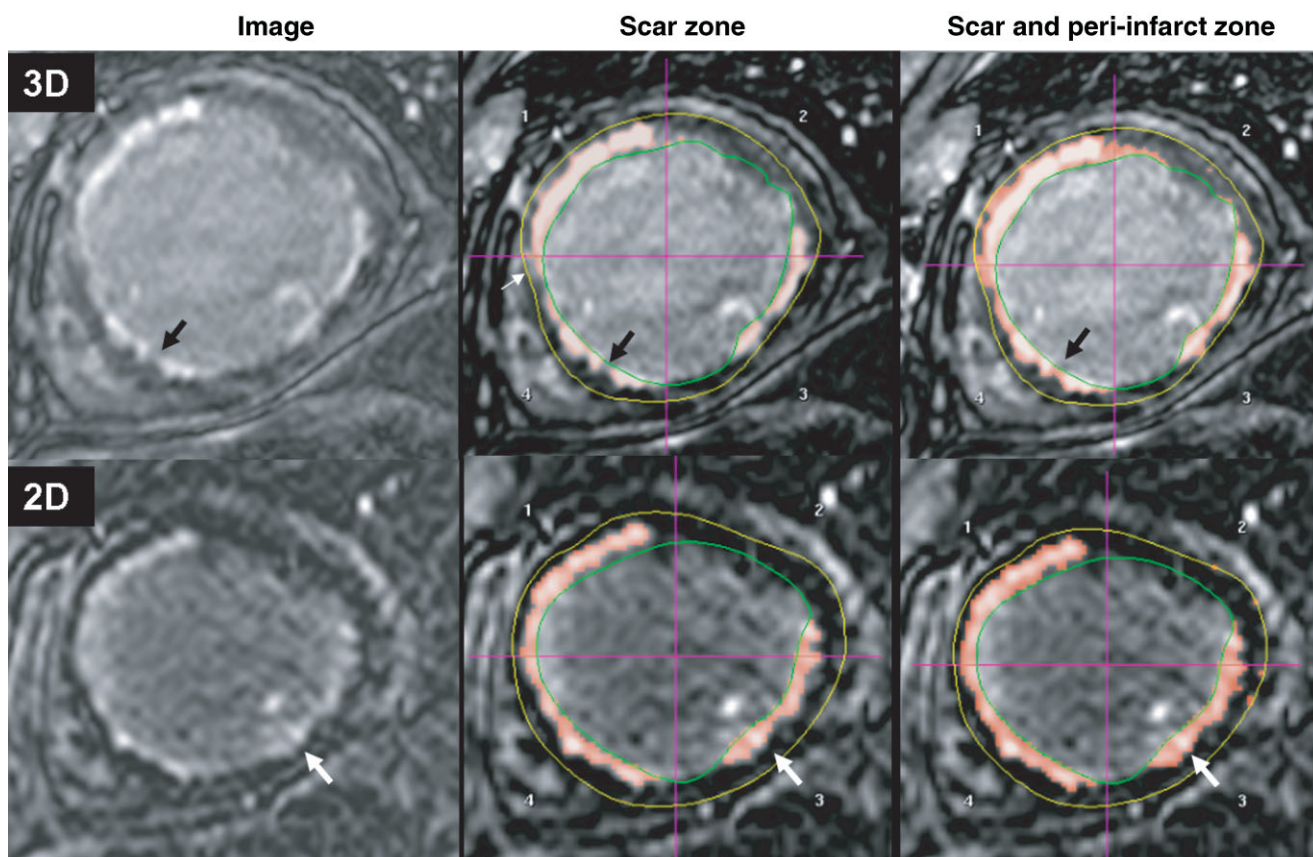
Image	Scar zone	Scar and peri-infarct zone

Figure 1. 3D and 2D LGE in matched slices in the same subject, showing the original images (left), and the identified scar (middle) and peri-infarct zone (right). For 2D LGE, the peri-infarct zone mainly lies along the border of the scar (white arrows). For 3D LGE, the peri-infarct zone also extends beyond the border (black arrows).

RESULTS

Subjects

Fourteen (four women, age 62 ± 11 years, LVEF 42 ± 12%) who met the inclusion criteria of prior myocardial infarction and at least average quality 2D and 3D LGE images that were positive for myocardial LGE on at least one scan comprised the final cohort of the study, out of 36 patients. Six patients were excluded due to lack of LGE. Sixteen patients were excluded due to low quality 3D LGE ($n = 12$, 33%) or nondiagnostic 3D LGE ($n = 4$, 15%) study. Low-quality scans were caused by ghosting and blurring or poor TI choice. Two nondiagnostic studies were caused by poor TI choice, and two for excessive ghosting and blurring. Because our purpose is to study the effects of spatial resolution on LGE imaging, these studies were excluded, since their spatial resolution was strongly modulated by motion blurring. For the remaining 14 patients, myocardial infarction was determined by EKG and positive enzymes ($n = 4$), catheterization ($n = 5$), or both ($n = 4$). One patient was diagnosed by LGE scar pattern. Four of the 14 patients had acute infarcts (<1 month). Patients were referred for assessment of LV function and viability ($n = 8$), scar characterization ($n = 5$), with one patient referred for LV function and aortic regurgitation. All data presented are from the final cohort of 14 patients.

Image Comparisons

Figure 2 shows comparisons of 2D and 3D images in matched slices for three subjects. Finer detail of LGE in the 3D images can be noted. Papillary muscle LGE in subjects 1 and 3 are more prominent on the 3D images, with the increase in spatial resolution provided by the 3D scans, and better display of the heterogeneity of the infarct. Figure 3A compares an image from a low-quality 3D LGE scan to the matched 2D LGE slice. The 2D LGE quality is higher, with greater image sharpness. However, the right ventricular infarction on 3D LGE is subjectively more prominent. Figure 3B shows matched slices for a study in which papillary LGE was detected on the 3D LGE, but not on the 2D LGE.

SNR and CNR and Subjective Quality

The LGE SNR, myocardial SNR, and papillary muscle-blood CNR were all significantly higher in the 3D LGE scans (Table 1). Using measured blood SNR and total scan times (including dead-times), the effective SNR efficiency ($SNR_{LGE}/Tscan^{1/2}$) was the same (ratio 2D/3D = 1.00) for the 2D and 3D scans. In the phantom study, the ratio of 3D to 2D SNR was 1.4 for the phantoms with T1s of 300 and 330 msec, which is similar to but greater than the ratio measured in vivo (1.3 and 1.1 for LGE and blood, respectively)

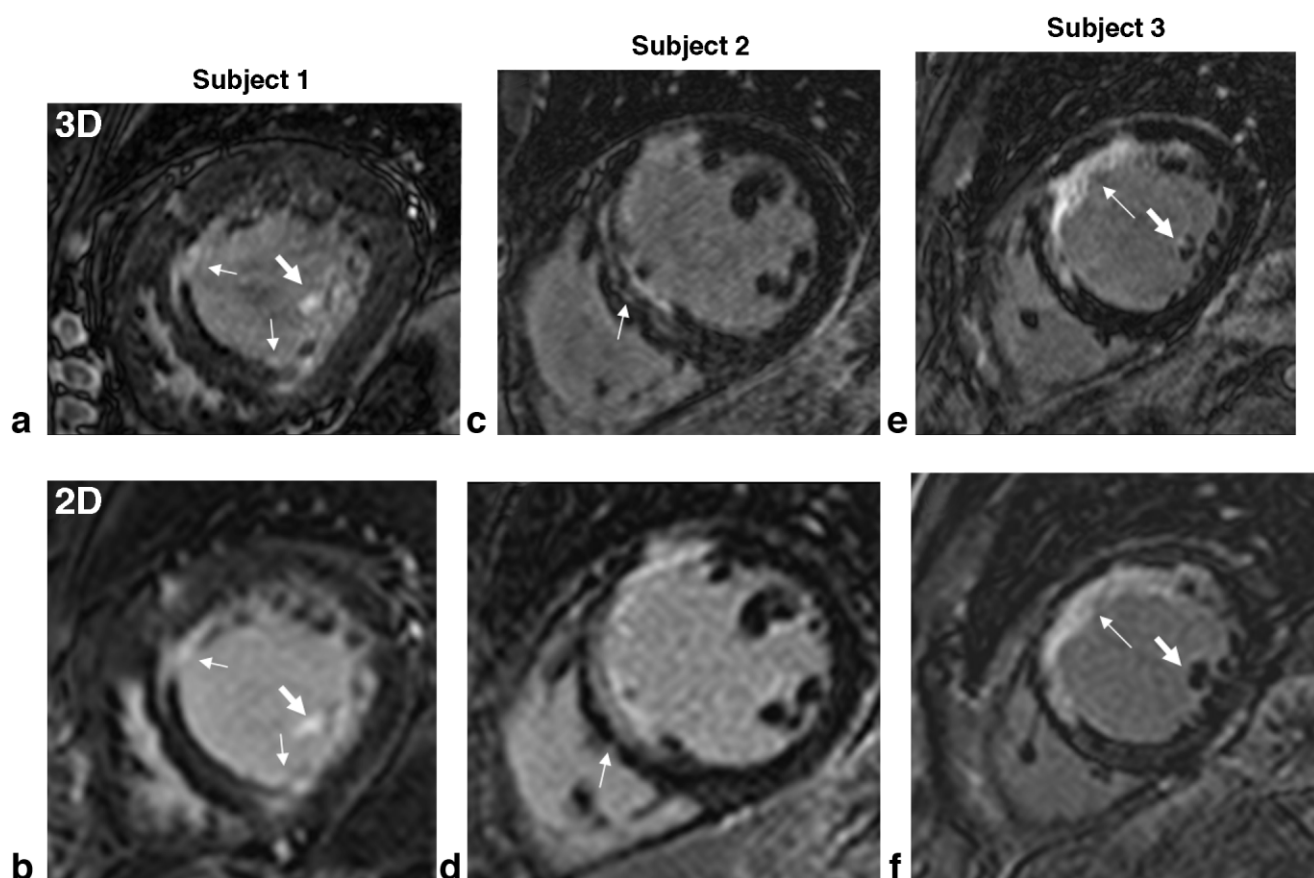Overall quality and contrast was graded as similar for the 2D and 3D LGE, but subjective sharpness was graded

Figure 2. Comparisons of 3D (a,c,e) and 2D (b,d,f) LGE in three subjects, showing higher spatial resolution provided by 3D LGE, illuminating an additional layer of complexity of myocardial scars (thin arrows). Subject 2 shows a double rim of scar (C, arrow), only suggested in (D). Papillary muscle LGE conspicuity is improved (fat arrows, subject 1). The 2D images of subject 3 (F) do not demonstrate papillary muscle LGE, but some LGE is observed in an adjacent 2D slice.

as 2.7 (fair to good) vs. 3.4 (good to excellent) for 2D and 3D LGE, respectively ($P < 0.001$) (Table 1). The interobserver agreement in overall quality was 60%, with a kappa value of 0.42, showing moderate agreement. A majority (9/14) of patients had heterogeneous LGE on 3D and 2D images. Of five patients with homogeneous scar, three had acute infarcts. Figures 2A–C and 3B are examples of LGE patterns with visually heterogeneous structure, while Fig. 3A is an example of a homogenous LGE.

Scar and Peri-Infarct Volume Measurements

Figure 4A and Table 2 compare total 2D and 3D LGE scar volume measurements, showing strong correlation. The 2D and 3D matched slice peri-infarct zone measurements are less strongly correlated (Fig. 4B, Table 2). A trend was found for larger measurements of peri-infarct volume using 3D LGE vs. 2D LGE for studies with heterogeneous LGE ($P = 0.15$, Table 2), and smaller peri-infarct volumes using 3D LGE vs. 2D LGE for studies with homogeneous LGE.

Papillary Muscle Scar

In 6/14 patients, papillary muscle scar was identified by 3D LGE. There was 2D/3D agreement about the presence of papillary scar in 13/14 cases; papillary scar

was confidently identified in one 3D LGE study, but not on the corresponding 2D LGE study. Furthermore, the observer had greater confidence in determining the presence of papillary LGE with 3D LGE (13/14 confidently determined on 3D vs. 7/14 on 2D, Table 1, $P = 0.008$). For the six patients with papillary muscle scar, the size of the papillary muscle/trabecular LGE was 9% and 6% that of the LV LGE on the 3D and 2D images, respectively (Table 2). Three patients had only anterolateral papillary muscle LGE (one with left circumflex artery infarct and another with three-vessel disease, another with left anterior descending artery infarct), and two patients had both posteromedial and anterolateral papillary LGE (one with three-vessel, another with LAD and LCx disease), and one (with multivessel disease) had only posteromedial papillary LGE. The presence of papillary muscle LGE was not significantly correlated with larger infarct size (15.0 ± 8.8 mL vs. 12.7 ± 8.6 mL, $P = 0.63$ with and without papillary muscle LGE) or LV dimensions or mass, but did correlate with mitral regurgitation fraction ($18.8 \pm 15.8\%$ vs. $5.1 \pm 5.5\%$, $P = 0.041$ with and without papillary muscle LGE), LVEF ($33 \pm 7.6\%$ vs. $48.8 \pm 9.9\%$, $P = 0.007$), and RVEF ($50.2 \pm 7.5\%$ vs. $63.0 \pm 6.0\%$, $P = 0.006$) as measured by cardiac MR.
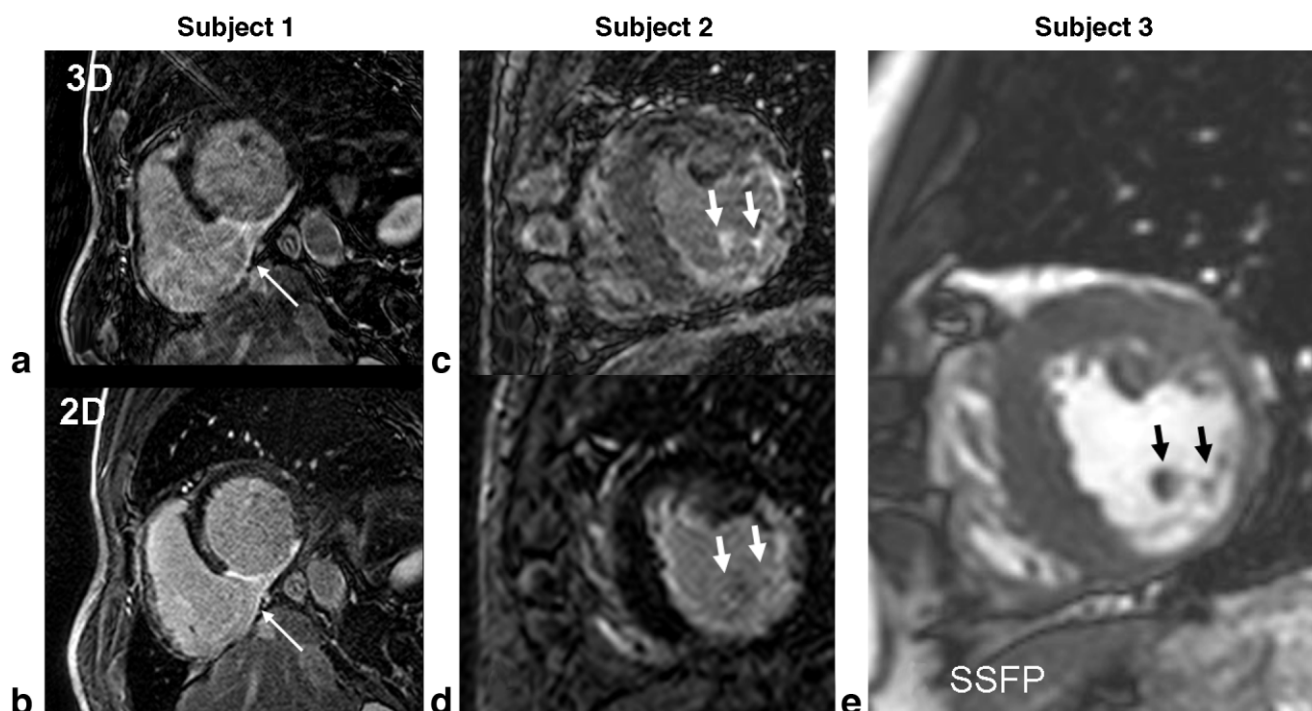
Subject 1   Subject 2   Subject 3

Figure 3. (**a**) Example of low-quality 3D, here caused by excessive motion artifacts, compared to the good-quality 2D LGE scan (**b**). Both images provide similar diagnostic information on inferior myocardial scar. The rare visualization of right ventricular infarct (arrow) is better observed in the lower-quality 3D scan, likely due to the thinner slices and longer delay postinjection. This patient has a homogeneous LGE structure. (**c**) 3D LGE with imperfect myocardial nulling. Papillary LGE (arrows) was observed in the 3D but not the 2D scan (**d**) in a patient with a heterogeneous LGE structure. Although no noninvasive gold standard exists for detection of papillary muscle scar, the presence of LGE in many slices of the 3D volume at the anatomic site of the papillary muscle (**e**, arrows) is compelling.

DISCUSSION

In this study of 14 subjects with prior myocardial infarction we found that higher spatial resolution 3D LGE provides greater sharpness and better ability to detect papillary muscle scar compared with standard 2D LGE.

Table 1
SNR and CNR, Image Quality, and Papillary Muscle LGE Detection

SNR and CNR (N=14)	2D	3D	P-value
LV LGE SNR	21 ± 8	29 ± 10*	<0.001
LV blood pool SNR	15 ± 9	16 ± 7	NS
LV myocardium SNR	2.2 ± 1.5	6.0 ± 3.8†	0.001
LV papillary LGE SNR	25 ± 22	31 ± 23	0.046
LGE-myocardium CNR	18 ± 7	20 ± 7	NS
Papillary LGE-blood CNR (N=6)	10 ± 8	14 ± 10‡	0.003
Subjective scorings (N=14) (1=poor, 4=Excellent)	2D	3D	3D
Overall quality	3.1	3.4	NS
Sharpness	2.7	3.4**	0.01
Contrast	3.7	3.4	NS
Papillary LGE present?	5/14	6/14	NS
High confidence for papillary LGE?	7/14	13/14***	0.008

SNR, signal-to-noise ratio; CNR, contrast-to-noise ratio; LGE, late gadolinium enhancement; LV, left ventricular; NS, nonsignificant.
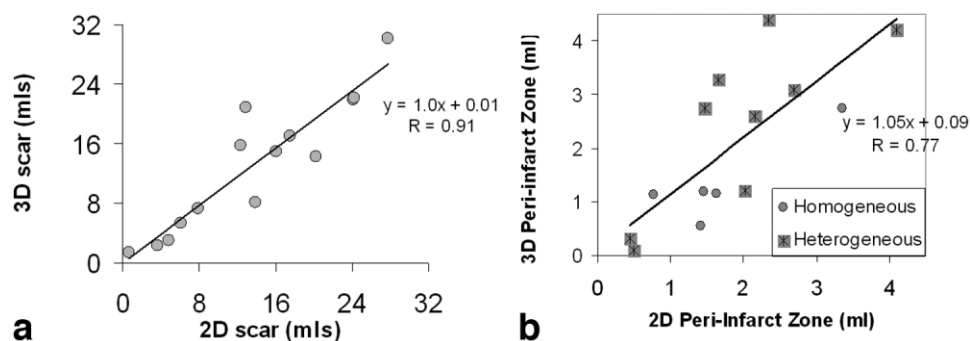
Scar Volumes

Scar volumes measured by the 2D and 3D LGE methods were in close agreement in our study, and consistent with data reported by others for 3D free-breathing LGE (15,16). Peri-infarct volume was also similar on 2D and 3D LGE, but there was a less strong correlation. The relative size of peri-infarct volume to scar volume in our study is similar to what has already been reported ((3–6). A recent animal study showed that one contributor to peri-infarct volume is partial volume averaging of edge voxels, which is reduced with higher spatial resolution (19). We found that scars with heterogeneous LGE structure had larger peri-infarct volumes on 3D LGE than 2D LGE ($P = 0.15$), while for patients with homogeneous scars the opposite held (3D LGE peri-infarct volume was less than by 2D LGE, $P = 0.015$). This trend, although not significant, may be the result of competing effects. 2D LGE measures a larger peri-infarct zone because its border pixels are larger, but gray zone is also the result of a heterogeneous structure, which 3D LGE is better able to demonstrate.

Papillary Muscle Scar

A large minority of our patients (42%) had 3D LGE evidence of papillary muscle scar, and this percentage agrees with an early study (20). Aside from LGE, no better standard exists except autopsy or surgery for

Figure 4. **a:** Comparison of 2D and 3D LGE volume measurements shows good agreement. **b:** Peri-infarct zone volume measured by 2D LGE and 3D LGE in a single 2D slice, matched with 3D slices, showing less correlation, with a trend toward larger peri-infarct volumes by 3D in more heterogeneous LGE.

detection of papillary scar. The SNR of papillary muscle LGE was higher than LV LGE for both 3D and 2D, likely due to partial volume averaging effects: myocardial LGE partial volumes with normal myocardium reducing its signal, while papillary LGE partial volumes with blood which does not reduce its signal as much as normal myocardium does. 3D LGE may be superior to 2D LGE in visualizing papillary muscle scar, as evidenced by higher SNRs, CNRs, increased papillary muscle scar volume, increased confidence of detection, and an instance of papillary muscle LGE that was not detected by 2D LGE (Fig. 3B). These data suggest that papillary muscle scar may be missed using standard spatial resolution 2D LGE approaches. The clinical role of the detection of papillary muscle scar by LGE is still unknown, but its detection may be important for diagnosis or treatment (21).

SNR and Image Quality of the 3D LGE Scans

The 3D LGE studies had higher LGE SNR compared to 2D, similar to the ratio of SNRs for phantoms. This is due to a combination of smaller voxel sizes, offset by greater averaging for 3D LGE. Furthermore, the longer delay between injection of contrast and imaging for 3D LGE (as 2D was always performed first) improves the LGE-to-myocardium contrast (22,23). The order was not randomized, as patients had been referred for clinical scanning and it was felt inappropriate to deviate from our clinical 2D LGE protocol. Myocardial nulling for 3D LGE was worse, possibly because a 2D LGE scan with poor nulling was repeated with an improved TI, while the 3D LGE was not, due to its lengthy acquisition. Differences in nulling may be the reason that scar SNR, but not CNR, was increased using 3D LGE. Overall image quality was similar. Finally, image sharpness

was significantly greater with the 3D LGE, which provided nominally 4× smaller voxels compared to 2D LGE. Future work should focus on improving the robustness of the 3D LGE technique, by reducing motion artifacts and improving the myocardial nulling, perhaps with a phase-sensitive inversion recovery method suitable for 3D free-breathing LGE.

Limitations

We compared the peri-infarct zone of a single 2D slice, matched to four 3D LGE slices. This permitted great care in contouring the slices to avoid inclusion of apical slices, and other slices where LGE cannot be distinguished from LV blood or artifacts. Since the threshold chosen for identifying the peri-infarct zone can easily influence the results, we chose thresholds that were less dependent on the SNR of the images, since we compared images with different SNRs (3D vs. 2D).

The higher spatial resolution 3D LGE scans was always performed about 7 minutes after the first 2D LGE breath-hold scan. This results in a greater T1 difference between scarred myocardium and blood (22,23) for the 3D LGE. We cannot exclude the influence of this on our findings of improved conspicuity of endocardial scar and papillary muscle and trabecular scar. 3D LGE also had smaller voxels and thinner slices. It is likely that all of these factors contributed to improved papillary muscle scar conspicuity on 3D LGE.

In conclusion, currently, in our experience, higher spatial resolution free-breathing 3D LGE provides sharper images and higher SNR, but worse myocardial nulling compared with 2D LGE. The overall image quality is similar. 3D LGE scar volumes are similar to those measured by 2D LGE, but peri-infarct volumes trend toward larger with 3D LGE for patients with heteroge-

Table 2
LGE Volumes

Volume (mL) (*N*=14)	2D	3D	Bias ±2 SD	R-value	*P*-value
Total LV (mL)	14.5 ± 8.2	13.2 ± 8.8	0.5 ± 6.8	0.91	0.59
LV papillary scar (*N*=6)	0.8 ± 1.0	1.2 ± 1.5	−0.5 ± 1.3		0.24
Single slice measurements*					
LV LGE (mL)	2.4 ± 1.7	2.2 ± 1.3	0.18 ± 1.5	0.91	0.38
Peri-infarct zone(all)* (mL)	1.9 ± 1.0	2.0 ± 1.4	−0.1 ± 0.9	0.77	0.40
Heterogeneous LGE (*N*=8)	1.9 ± 1.1	2.4 ± 1.6	−0.39 ± 1.0	0.79	0.15
Homogeneous LGE (*N*=6)	1.7 ± 1.0	1.3 ± 0.8	0.37 ± 0.5	0.88	0.15

LGE, late gadolinium enhancement; LV, left ventricular.
*Measured in a single 2D LGE slice, compared to four 3D LGE slices.

neous scars. 3D LGE, and imaging at longer delays postcontrast injection, may be superior in visualization of the common finding of papillary muscle scar, but this must be confirmed in a larger study.

REFERENCES

1. Kim RJ, Wu E, Rafael A, et al. The use of contrast-enhanced magnetic resonance imaging to identify reversible myocardial dysfunction. N Engl J Med 2000;343:1445–1453.
2. Simonetti OP, Kim RJ, Fieno DS, et al. An improved MR imaging technique for the visualization of myocardial infarction. Radiology 2001;218:215–223.
3. Nazarian S, Bluemke DA, Lardo AC, et al. Magnetic resonance assessment of the substrate for inducible ventricular tachycardia in nonischemic cardiomyopathy. Circulation 2005;112:2821–2825.
4. Yan AT, Shayne AJ, Brown KA, et al. Characterization of the peri-infarct zone by contrast-enhanced cardiac magnetic resonance imaging is a powerful predictor of post-myocardial infarction mortality. Circulation 2006;114:32–39.
5. Bello D, Fieno DS, Kim RJ, et al. Infarct morphology identifies patients with substrate for sustained ventricular tachycardia. J Am Coll Cardiol 2005;45:1104–1108.
6. Schmidt A, Azevedo CF, Cheng A, et al. Infarct tissue heterogeneity by magnetic resonance imaging identifies enhanced cardiac arrhythmia susceptibility in patients with left ventricular dysfunction. Circulation 2007;115:2006–2014.
7. Kwong RY, Chan AK, Brown KA, et al. Impact of unrecognized myocardial scar detected by cardiac magnetic resonance imaging on event-free survival in patients presenting with signs or symptoms of coronary artery disease. Circulation 2006;113:2733–2743.
8. Bogun F, Desjardins B, Crawford T, et al. Post-infarction ventricular arrhythmias originating in papillary muscles. J Am Coll Cardiol 2008;51:1794–1802.
9. Han Y, Peters D, Salton C, et al. Cardiovascular magnetic resonance characterization of mitral valve prolapse. J Am Coll Cardiol Imaging 2008;1:294–303.
10. Good E, Desjardins B, Jongnarangsin K, et al. Ventricular arrhythmias originating from a papillary muscle in patients without prior infarction: a comparison with fascicular arrhythmias. Heart Rhythm 2008;5:1530–1537.
11. Goldfarb J, Shinnar M. Free-breathing contrast-enhanced MR imaging of myocardial dysfunction: clinical application of real-time navigator echo imaging. In: Proc 10th Annual Meeting ISMRM, Honolulu; 2002:1640.
12. Kuhl HP, Papavasiliu TS, Beek AM, Hofman MB, Heusen NS, van Rossum AC. Myocardial viability: rapid assessment with delayed contrast-enhanced MR imaging with three-dimensional inversion-recovery prepared pulse sequence. Radiology 2004;230:576–582.
13. Dewey M, Laule M, Taupitz M, Kaufels N, Hamm B, Kivelitz D. Myocardial viability: assessment with three-dimensional MR imaging in pigs and patients. Radiology 2006;239:703–709.
14. Foo TK, Stanley DW, Castillo E, et al. Myocardial viability: breath-hold 3D MR imaging of delayed hyperenhancement with variable sampling in time. Radiology 2004;230:845–851.
15. Nguyen TD, Spincemaille P, Weinsaft JW, et al. A fast navigator-gated 3D sequence for delayed enhancement MRI of the myocardium: comparison with breathhold 2D imaging. J Magn Reson Imaging 2008;27:802–808.
16. Saranathan M, Foo T, Castillo E, Hoppel B, Wu K. Fast three-dimensional, free-breathing imaging of myocardial infarction. In: Proc 10th Annual Meeting ISMRM, Honolulu; 2002:1623.
17. Look D, Locker D. Time savings in measure of NMR and EPR relaxation times. Rev Sci Instrum 1970;41:250–251.
18. Amado LC, Gerber BL, Gupta SN, et al. Accurate and objective infarct sizing by contrast-enhanced magnetic resonance imaging in a canine myocardial infarction model. J Am Coll Cardiol 2004;44:2383–2389.
19. Hsu L-Y, Schelbert E, Anderson SA, et al. Delayed enhancement of the peri-infarct border zone is significantly affected by partial volume averaging: insights from ex vivo rat heart images at near-cellular resolution. In: Proc 16th Annual Meeting ISMRM, Toronto; 2008:2953.
20. Kron IL, DiMarco JP, Lerman BB, Nolan SP. Resection of scarred papillary muscles improves outcome after surgery for ventricular tachycardia. Ann Surg 1986;203:685–690.
21. Harrigan CJ, Appelbaum E, Maron BJ, et al. Significance of papillary muscle abnormalities identified by cardiovascular magnetic resonance in hypertrophic cardiomyopathy. Am J Cardiol 2008;101:668–673.
22. Goldfarb JW, Mathew ST, Reichek N. Quantitative breath-hold monitoring of myocardial gadolinium enhancement using inversion recovery TrueFISP. Magn Reson Med 2005;53:367–371.
23. Klein C, Nekolla SG, Bengel FM, et al. Assessment of myocardial viability with contrast-enhanced magnetic resonance imaging: comparison with positron emission tomography. Circulation 2002;105:162–167.